Operando characterisation of alumina-supported bimetallic Pd–Pt catalysts during methane oxidation in dry and wet conditions

Large, A. ORCID: https://orcid.org/0000-0001-8676-4172, Seymour, J. ORCID: https://orcid.org/0000-0002-1217-9541, Quevedo Garzon, W., Roy, K. ORCID: https://orcid.org/0000-0003-0802-7710, Venturini, F., Grinter, D. C. ORCID: https://orcid.org/0000-0001-6089-119X, Artiglia, L. ORCID: https://orcid.org/0000-0003-4683-6447, Brooke, E., de Gutierrez, M. B., Raj, A., Lovelock, K. R. J. ORCID: https://orcid.org/0000-0003-1431-269X, Bennett, R. A. ORCID: https://orcid.org/0000-0001-6266-3510, Eralp-Erden, T. and Held, G. ORCID: https://orcid.org/0000-0003-0726-4183
(2021) Operando characterisation of alumina-supported bimetallic Pd–Pt catalysts during methane oxidation in dry and wet conditions. Journal of Physics D: Applied Physics, 54 (17). 174006. ISSN 1361-6463 doi: https://doi.org/10.1088/1361-6463/abde67 Available at http://centaur.reading.ac.uk/96558/

Journal of Physics D: Applied Physics

PAPER • **OPEN ACCESS**

Operando characterisation of alumina-supported bimetallic Pd–Pt catalysts during methane oxidation in dry and wet conditions

To cite this article: Alexander Large *et al* 2021 *J. Phys. D: Appl. Phys.* **54** 174006

OPEN ACCESS
IOP Publishing
Journal of Physics D: Applied Physics
J. Phys. D: Appl. Phys. **54** (2021) 174006 (10pp)
https://doi.org/10.1088/1361-6463/abde67

Operando characterisation of alumina-supported bimetallic Pd–Pt catalysts during methane oxidation in dry and wet conditions

Alexander Large[1,2,3], Jake Seymour[1], Wilson Quevedo Garzon[2], Kanak Roy[2], Federica Venturini[2], David C Grinter[2], Luca Artiglia[4], Emily Brooke[3], Martha Briceno de Gutierrez[3], Agnes Raj[3], Kevin R J Lovelock[1], Roger A Bennett[1], Tugce Eralp-Erden[3] and Georg Held[1,2]

[1] University of Reading, Reading RG6 6AD, United Kingdom
[2] Diamond Light Source, Harwell Campus, Didcot OX11 0QX, United Kingdom
[3] Johnson Matthey Technology Centre, Sonning Common RG4 9NH, United Kingdom
[4] Swiss Light Source, Forschungsstraße 111, 5232 Villigen PSI, Switzerland

E-mail: georg.held@diamond.ac.uk

Received 4 October 2020, revised 11 December 2020
Accepted for publication 21 January 2021
Published 16 February 2021

Abstract

Near ambient pressure x-ray photoelectron spectroscopy (NAP-XPS) was used to study the chemical states of a range of alumina-supported monometallic Pd and bimetallic Pd–Pt nanocatalysts, under methane oxidation conditions. It has been suggested before that for optimal complete methane oxidation, palladium needs to be in an oxidised state. These experiments, combining NAP-XPS with a broad range of characterisation techniques, demonstrate a clear link between Pt presence, Pd oxidation, and catalyst activity under stoichiometric reaction conditions. Under oxygen-rich conditions this behaviour is less clear, as all of the palladium tends to be oxidised, but there are still benefits to the addition of Pt in place of Pd for complete oxidation of methane.

Supplementary material for this article is available online

Keywords: methane oxidation, ambient-pressure XPS, palladium, heterogeneous catalysis, platinum

(Some figures may appear in colour only in the online journal)

1. Introduction

Natural gas engines continue to offer a viable green alternative to traditional petrol and diesel engines, as they produce significantly lower quantities of carbon dioxide. Unfortunately, unburnt methane persists in the exhaust feed and poses a potential problem as a greenhouse gas. In addition, continually tightening regulations require reduction in methane emissions from petrol engine vehicles across all classes. This necessitates improved exhaust treatment catalysts to convert the remaining methane to cleaner products such as CO_2 and H_2O.

$$CH_4 + 2O_2 \rightarrow 2H_2O + CO_2. \quad (1)$$

Platinum group metals (PGM) are widely used as catalysts for a variety of reactions. Both Pd and Pt have been used

for complete and partial methane oxidation, whereby Pd is understood to be the more active metal for the reaction [1–5]. Studies conducted to better understand the active state of Pd methane oxidation catalysts generally agree that a mixture of metal and oxide is necessary for optimum performance [6–9]. For both metals a strong particle size effect has been demonstrated [10]. A combined experimental and theoretical study of palladium single crystal surfaces showed that both metallic palladium and palladium oxide were preferable to thin layers of oxide over a metallic bulk [11].

A key issue in the use of palladium (oxide) as a catalyst for methane combustion is that the catalyst is deactivated by water [12–15]. This is made worse by the reaction itself, which produces water.

Previous experiments have shown $Pd(OH)_2$ forming in preference to PdO under methane oxidation conditions on alumina, although the opposite preference was found on tin oxide. The suggestion presented was that this is due to hydroxyls forming more easily on alumina, which can then provide them to the Pd [16]. Variation in support can have a substantial effect on the deactivation in wet conditions. This has been attributed to the varying hydrophobicity of the supports, which can prevent the build-up of hydroxyls on the support surface [17]. Alumina supported catalysts have been doped in an attempt to reduce the inhibition effects of water. Alyani *et al* doped the Pd/Al_2O_3 catalyst with ceria, and demonstrated that this reduces the amount of water which adsorbs on the surface [18]. Zeolites have shown promise as a support, due to the potential for tuning the hydrophilic/hydrophobic nature by varying the silica/alumina ratio. Losch *et al* produced an effective Pd/zeolite catalyst for methane combustion in wet conditions using this approach [19].

Murata *et al* showed how changing the support can alter the Pd nanoparticle structure, with the best supports (such as alumina and ceria) preserving the nanoparticle in a metallic core and oxidised shell structure [20]. The same group had previously reported how the optimal palladium particle size varied with different supports [21].

Another suggestion for limiting the water deactivation effects was to use bimetallic Pd–Pt catalysts instead of pure palladium [22, 23]. The addition of platinum has also been shown to be beneficial for long term catalytic stability [24–29] and enhancing the resistance to sulfur poisoning, which is a significant problem for exhaust catalysts [30, 31]. In addition, platinum is a significantly less expensive metal than palladium (by more than 60% based on recent values) gram for gram. As such, replacing even small amounts of palladium with platinum can be hugely beneficial, when catalysts are produced on a large scale. Recently, Martin *et al* used in-situ x-ray absorption spectroscopy (XAS) to show that activity is optimised when PdO is formed on the surface of bimetallic Pd–Pt nanoparticles [32]. This study also found that, for samples prepared at 500 °C (as those presented here), Pt is still present at the surface. A related study demonstrated a significant increase in PdO with increasing oxygen concentrations in the gas feed [33]. Whilst the deactivation effects are seen, there is not yet a complete understanding of the effects platinum has on palladium under these conditions. Goodman *et al* demonstrated that Pd–Pt catalysts with no PdO phase were significantly worse than Pd catalysts in terms of initial reaction rate, but did not significantly suffer from deactivation by water [34]. Velin *et al* studied surface hydroxyl formation and suggested the formation of hydroxyls at the $PdO\text{-}Al_2O_3$ boundary was responsible for the decrease in activity in wet conditions [17].

Clearly, as heterogeneous catalysis is fundamentally a surface process, more quantitative information about the chemical composition near the surface is essential for a better understanding of these catalysts at the atomic level. Recent developments in near-ambient pressure x-ray photoelectron spectroscopy (NAP-XPS) have enabled surface-specific quantitative, chemical analysis under gas atmospheres of a few mbar, thereby bridging the 'pressure gap' between traditional vacuum-based surface science measurements and the pressures of catalytic reactors. NAP-XPS can therefore help to determine oxidation states and identify active surface species under reaction conditions and thus significantly contribute to addressing the role of Pt in methane oxidation catalysis.

Recently, our group used NAP-XPS to study the surface composition of Pd/Al_2O_3 catalysts under partial methane oxidation conditions [35]. We could show a correlation between the oxidation of palladium and the production of CO, followed by reduction of the palladium occurring during H_2 production.

In the present study we investigate bi-metallic Pd–Pt catalysts for complete oxidation of methane. Whilst many studies claim that an oxidised palladium surface yields the highest activity for complete methane oxidation there is little evidence from our *in situ* studies to support this conclusion. By performing NAP-XPS studies of a series of $Pd\text{–}Pt/Al_2O_3$ catalysts with different Pd:Pt ratios, we observe significant changes in the oxidation state of palladium depending on the reaction conditions and the concentration of platinum.

2. Experimental

2.1. Sample preparation

A range of $Pd\text{–}Pt/Al_2O_3$ samples were prepared by incipient wetness impregnation, using $Pd(NO_3)_2$ and $Pt(NO_3)_2$ precursors [36]. The solutions were combined and added to $\gamma\text{-}Al_2O_3$. The resulting mixtures were dried for 4 h at 120 °C, then calcined in air for 2 h at 500 °C. For the synchrotron studies, 1 g of the catalyst powders was mixed with 3 g of water and 0.1 g of Disperal P3. The mixtures were drop cast onto silicon wafers (Si(100) with a 100 nm layer of gold on the reverse side), which were heated after deposition to leave a dry catalyst layer. Excess powder was removed from the wafer, to leave a thin layer of sample. Platinum and palladium loadings are referred to throughout as weight percentages relative to alumina support. A full list of compositions produced, along with the particle sizes as determined by CO chemisorption experiments, is presented in table 1.

2.2. Initial sample characterisation

The catalyst surface composition was initially characterised using a Thermo Escalab 250 laboratory XPS instrument with

Table 1. PGM particle sizing of all bimetallic and monometallic catalysts after treatment at 500 °C and 900 °C. Treatments performed for 2 h in a static air ager. 900 °C treated samples were previously treated at 500 °C for 2 h. The change in size as determined by CO chemisorption is also shown. Quoted particle sizes are average particle diameters as determined by CO chemisorption measurements. TEM particle sizes quoted as average diameter with standard deviation. Composition values based on amounts of precursor solution used. Active sites values are as determined by CO chemisorption. Note, unless stated, activity measurements and NAP-XPS experiments were performed with catalysts calcined at 500 °C.

		Size (nm)			TEM size	
Composition wt.%	At. ratio Pd:Pt	500 °C	900 °C	Change (nm)	500 °C	Active sites (mol g^{-1})
1.0Pd	—	5.0	8.5	3.5	—	7.84×10^{-6}
2.5Pd	—	15.4	12.3	−3.1	—	6.39×10^{-6}
4.0Pd	—	19.1	18.2	−0.9	—	8.23×10^{-6}
5.0Pd	—	14.7	28.0	13.3	12 ± 5	1.34×10^{-5}
4.0Pd–1.0Pt	7.33:1.00	14.4	29.1	14.7	9 ± 5	1.25×10^{-5}
2.5Pd–2.0Pt	2.29:1.00	10.6	35.6	25.0	—	1.34×10^{-5}
2.5Pd–2.5Pt	1.83:1.00	10.5	52.7	42.2	6 ± 5	1.46×10^{-5}
2.5Pd–3.0Pt	1.53:1.00	9.0	38.6	29.6	—	1.83×10^{-5}
1.0Pd–4.0Pt	0.46:1.00	4.0	50.2	46.2	1.3 ± 0.4	3.13×10^{-5}
1.0Pt	—	2.4	28.6	26.3	—	9.22×10^{-6}
2.5Pt	—	2.4	44.2	41.8	—	2.26×10^{-5}
4.0Pt	—	2.6	29.9	27.3	—	3.35×10^{-5}
5.0Pt	—	2.6	75.9	73.3	1.2 ± 0.5	4.19×10^{-5}

a monochromatised Al Kα source (hv = 1486.6 eV). The catalyst powders were mounted onto carbon tape, and a flood gun was utilised for charge compensation.

Surface area, particle size, active sites and dispersion are calculated from CO chemisorption experiments, performed on a Micromeritics Autochem II 2920. 0.4 g of each sample was used, and initially reduced in H_2 at 300 °C for 30 min. The sample was cooled, and CO pulsed, with the amount of CO adsorbed measured, and used to determine the active surface area of the sample. From this, and knowledge of the amount of platinum group metal(s) (PGM) present, the dispersion and particle size were determined. This method assumes particles are hemispherical and equal in size, and as such it is only used as a general estimate to show trends.

Additional particle size measurements were conducted using a JEM 2800 transmission electron microscope at 200 kV and 40 μm C2 aperture. Samples were ground between two glass slides and dusted onto holey carbon coated copper TEM grid. Dark-field (Z-contrast) imaging was performed in scanning mode using an off-axis annular detector, with compositional analysis performed by x-ray emission detection in scanning mode. Particle size analysis performed on at least 60 different particles from a single image.

Most activity testing was conducted with catalysts calcined at 500 °C using a batch flow reactor. Catalyst powders were pressed into pellets, crushed and sieved between 250 and 355 μm. 0.4 g of the catalyst pellets were placed into the reactor bed and 0.1% of methane was flowed, with either 0.2% oxygen, 1% oxygen, 12% oxygen, 0.2% oxygen and 10% water, or 12% oxygen and 10% water (balanced with nitrogen to a total pressure of 1 mbar in all cases), with the temperature ramped from 150 °C up to a maximum of 590 °C at a rate of 15 °C min^{-1}. Gas composition analysis is conducted by FTIR, and methane conversion was measured by the change in concentration of methane in the output gas stream. Product selectivity was determined by measuring the concentration of carbon dioxide, water, carbon monoxide and hydrogen. Values for T20, T50 and T90 (the temperatures at which 20%, 50% and 90% conversion are reached respectively) are included for all catalytic tests in the supporting information (available online at stacks.iop.org/JPD/54/174006/mmedia) in table S1. Turnover frequencies of catalysts are determined at 250 °C and 350 °C under dry and wet conditions respectively. The methane conversion at that temperature is multiplied by the flow rate of methane through the reactor to determine the molar conversion rate of methane at that temperature. This conversion is then divided by the molar amount of active sites, as determined by CO chemisorption, to give the turnover frequency (TOF).

Support and nanoparticle phases were studied by powder x-ray diffraction (XRD), using a Bruker D8 Advance. Cu Kα radiation, 10°–130° 2θ, step size of 0.044°, tube voltage and current of 40 kV and 40 mA respectively.

2.3. Synchrotron experiments

2.3.1. NAP-XPS synchrotron experiments. For the near-ambient pressure XPS measurements only catalysts treated at 500 °C were used. NAP-XPS data were recorded at the B07 VerSoX beamline of Diamond Light Source, unless otherwise stated [37]. The spectra presented here were recorded with a photon energy of 1350 eV, an exit slit gap of 50 μm, and a pass energy of 20 eV. The samples were initially characterised at room temperature in vacuum ($<10^{-6}$ mbar, labelled as 'UHV') to verify the oxidation state of the metals before the reaction. The chamber was then filled with the reactant gases, the ratios of which varied in different experiments. The gas ratios used are summarised in table 2. Initial experiments were performed with a mixture of methane and oxygen ('dry stoic.'; ratio 1:2; total pressure 0.33 mbar) or methane, oxygen and water ('wet stoic.'; ratio 1:2:2; total pressure 0.55 mbar and 'very wet stoic.'; ratio 1:2:100; total pressure 5.2 mbar).

Table 2. Gas conditions used in the NAP-XPS experiments, including the relative gas ratios and the total pressures used. The methane partial pressure was kept the same, 0.11 mbar, in all experiments; the partial pressures of oxygen and water were adjusted accordingly to achieve the desired gas ratios. Activity refers to gas compositions that were also used during catalytic activity tests. For activity tests, methane is present at 1000 ppm, with nitrogen used to achieve 1 bar total pressure for all compositions.

Gas Condition	CH_4	O_2	H_2O	NAP (mbar)	Activity
Dry stoichiometric	1	2	—	0.33	Yes
Wet stoichiometric	1	2	2	0.55	No
SLS wet stoichiometric	1	2	15–28[a]	1.20	No
Very wet stoichiometric	1	2	100	5.20	Yes
Dry oxygen rich	1	120	—	2.90	Yes
Wet oxygen rich	1	120	100	5.20	Yes

[a] SLS refers to experiments performed at Swiss Light Source, where the water partial pressure varied between samples.

The 'dry' and 'very wet' stoichiometric conditions match the gas ratios which are used for catalytic activity tests. Additional experiments were carried out in more oxygen-rich feeds, which used a mixture of methane and oxygen ('dry rich'; ratio 1:120; total pressure 2.9 mbar) or methane, oxygen and water ('wet rich'; ratio 1:120:100; total pressure 5.2 mbar). These experiments provided NAP-XPS data for gas ratios which activity data had been collected for.

Additional NAP-XPS experiments were performed on the AP-XPS endstation of the X07DB *In Situ* Spectroscopy beamline at Swiss Light Source [38, 39]. All spectra from this beamtime were recorded at 900 eV. Total gas pressure of approx. 1.2 mbar was achieved, with a gas ratio of methane, oxygen and water of approx. 1:2:20.

Spectra were typically recorded at 50 °C intervals from 177 °C to 477 °C. The selected temperatures varied between samples depending on where significant activity changes occurred. A mass spectrometer located in the differential pumping system allowed for monitoring of reaction products.

2.3.2. XPS data analysis. In order to compensate for charging-related energy shifts, the energy axes of all spectra were calibrated with respect to the main Al 2p peak at 74.6 eV. Normalisation and background removal was applied at the low binding-energy side of each spectrum. Where differential sample charging was observed, multiple Al 2p peaks were fitted, and the same line shape was used to fit the relevant palladium spectra, as our group has previously reported [35]. Palladium spectra were fitted based on Pd $3d_{5/2}$ peaks at 335.0 (Pd(0)) and 336.5 (Pd(II)) eV respectively. Peak positions were restricted to binding energies within ±0.2 eV of the above values in order to ensure consistency across all data sets. In some cases this leads to non-perfect fits of the experimental data. An example of the fitting procedure is shown in figures S1 and S2 of the supporting information. An example survey spectrum is shown in figure S7, showing minimal contamination. Platinum spectra are not shown for any NAP-XPS experiments. The most intense Pt peaks (4f) appear at 71.0 and 72.4 eV, strongly overlapping with the most intense Al peak (2p) which is at 74.6 eV and broader. Al is present in significantly higher quantity than Pt for the powder catalysts. In theory these peaks could be fitted with the Al 2p spectra, but the errors this would introduce are too large for the results to be meaningful. Pt 4d peaks ($4d_{5/2}$ at 315, $4d_{3/2}$ at 332 eV) could be used, but due to the low cross section, large peak width and low concentration of Pt in the samples these peaks were never resolved well enough to yield useful information. In order to study the link between the oxidation states of Pd and Pt in bimetallic systems we prepared layered Pd–Pt model systems and studied them separately in vacuum.

The values of Pd(II) % as quoted in the text are shown for all samples and conditions in table S2 of the supporting information, with additional data from Swiss Light Source presented in figure S3.

3. Results and discussion

Transmission electron microscopy measurements with electron dispersive x-ray spectroscopy (TEM-EDX) are shown in figure 1. Additional EDX data are shown in the supporting information in figures S4 and S5. XRD data for select catalysts, confirming the phases of the support and nanoparticles, are shown in figure S6. Catalyst composition values are referred to throughout based on the weight (wt.) % of Pd and Pt. The corresponding atom (at.) % are shown in table 1, and show that even for a 2.5Pd–2.5Pt (wt. %) catalyst, the atomic ratio of Pd:Pt is 1.83:1, i.e. for all bimetallic catalysts presented and discussed in detail, Pd is the major PGM component. These images show that calcination at 500 °C produces bimetallic nanoparticles. This is true for both studied compositions (4.0Pd–1.0Pt and 2.5Pd–2.5Pt). There is no clear structuring to the particles (i.e. core–shell), with both metals present throughout the particles. From our experiments, the higher temperature calcination does not affect particle composition, but does still lead to an increase in particle size. Particle size analysis was performed with further TEM imaging, along with CO chemisorption measurements. These data are summarised in table 1.

From CO chemisorption, it is clear that there is a significant difference in particle sizes for catalysts of different compositions. A full list of average sizes is shown in table 1; after calcination at 500 °C they vary between 2.6 nm for 5.0Pt and 19.1 nm for 4.0Pd. The lower particle size for Pt compared to Pd can partially, but not fully, be attributed to the lower atomic loading of Pt (by a factor 1.83), as compositions were based on weight loading. A decrease in average may be expected for the bimetallic samples, as platinum forms smaller particles than palladium. The particle sizes for the higher loadings of monometallic palladium, 2.5Pd, 4.0Pd, and 5.0Pd, are all in a similar range, 14.7–19.1 nm. The distribution of sizes for this range of loading is within the error margin of the CO chemisorption method, so there is not a clear trend. There is, however, a significant change in average size for the low loading 1.0Pd monometallic samples, with average particle size of 5.0 nm. Platinum particles are largely equal in size, 2.5 nm ± 0.1 nm, despite variation in loading. Calcination at 900 °C increases

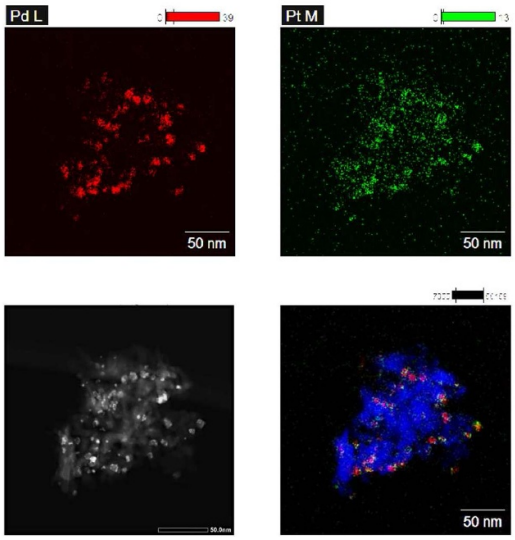

(a) TEM image and EDX maps for 4.0Pd-1.0Pt catalyst.

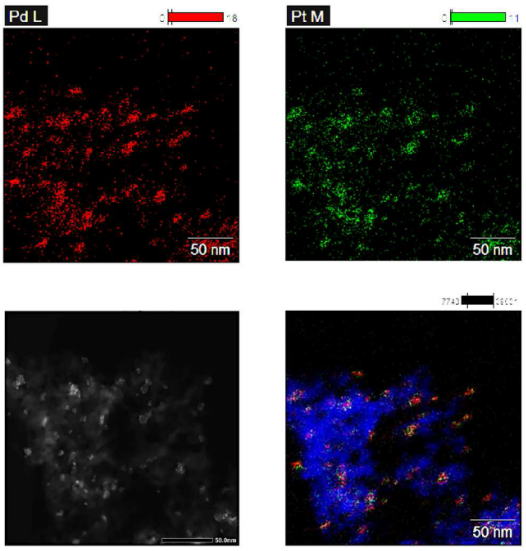

(b) TEM image and EDX maps for 2.5Pd-2.5Pt catalyst.

Figure 1. EDX maps for (clockwise from top left) Palladium, Platinum, and Pd–Pt overlaid with aluminium (blue) for various catalysts. Dark field TEM images (bottom left) for each catalyst. All scale bars 50 nm.

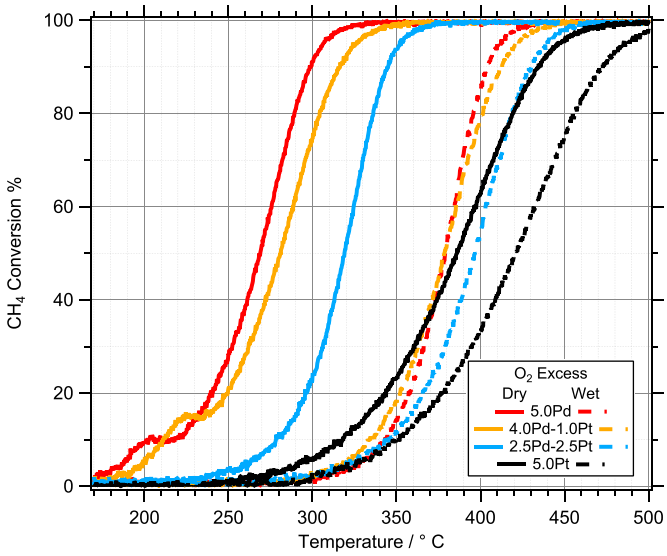

(a) CH_4:O_2:H_2O 1:120(:100)

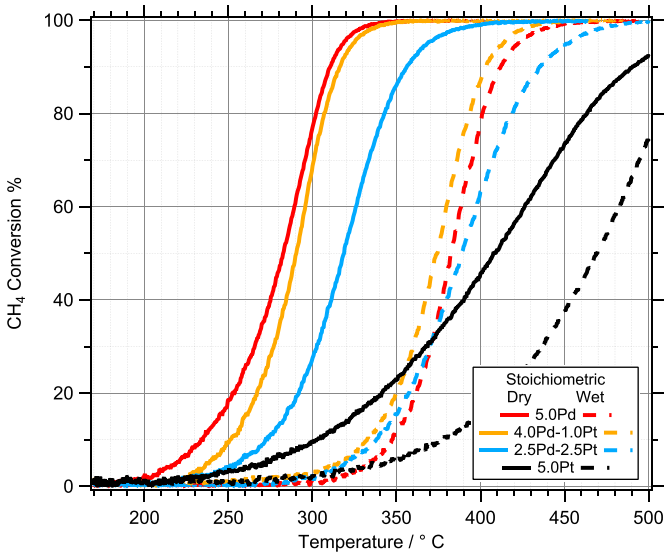

(b) CH_4:O_2:H_2O 1:2(:100)

Figure 2. Complete methane oxidation light off curves under various conditions: (a) CH_4:O_2:H_2O = 1:120(:100) and (b) CH_4:O_2:H_2O = 1:2(:100) for a range of monometallic and bimetallic catalysts calcined at 500 °C.

particle sizes for all compositions, in particular monometallic Pt. Now, an overall trend of increasing size with increased loading is observed (with outliers at 2.5/4.0Pt) and a higher Pt content generally leads to larger particles, in contrast to the observations after treatment at 500 °C. Due to this large increase in particle size for calcination at 900 °C, only catalysts calcined at 500 °C were used for the activity and NAP-XPS measurements presented below.

Catalytic activity plots for a series of mono- and bimetallic catalysts are presented in figure 2, under both oxygen-rich and stoichiometric conditions, with and without water. Under both stoichiometric and oxygen rich dry conditions, the 5.0 wt.% Pd catalyst (‘5.0Pd’) shows activity at the lowest temperature. The activity curves for 5.0Pd and 4.0Pd–1.0Pt under oxygen-rich conditions show shoulders at 200 °C and 220 °C, respectively, which are also observed for lower monometallic Pd loadings. As these are reproducible and the activity is stable over time at these temperatures, they indicate a reversible transformation (chemical or structural) of the catalyst at the onset of the reaction. Under stoichiometric wet conditions, the 4.0 wt.% Pd + 1.0 wt.% Pt catalyst (‘4.0Pd–1.0Pt’) is active at lower temperatures than the 5.0Pd. The deactivation, measured by the difference in T50 between dry and wet conditions, is consistently higher for 5.0Pd (110 °C and 100 °C respectively) than for 4.0Pd–1.0Pt (98 °C and 84 °C respectively). These values continually decrease as the catalyst composition becomes more Pt-rich. At the same time T50 rises, i.e. the overall activity decreases

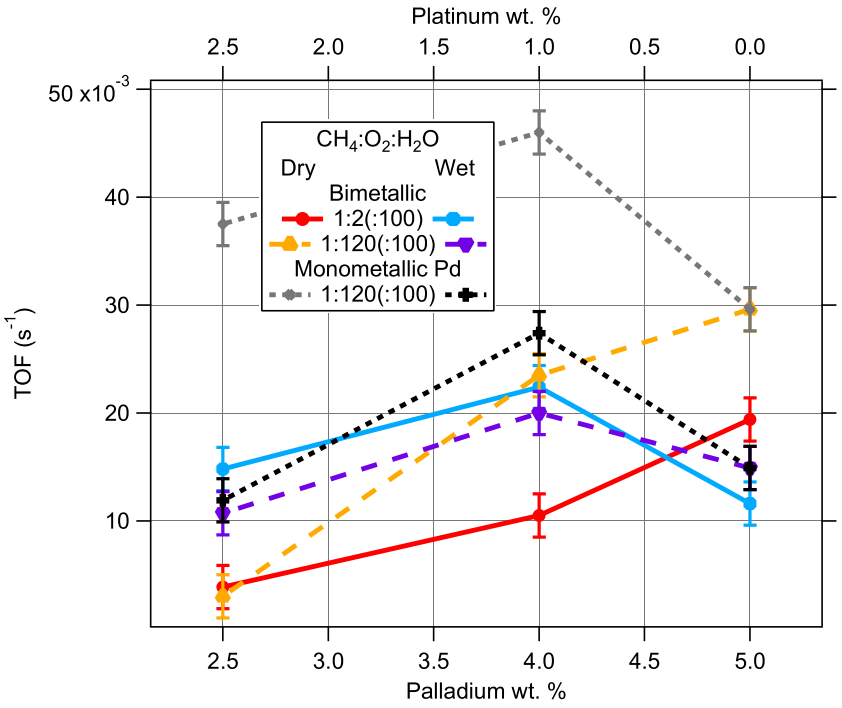

Figure 3. Turnover frequency (TOF) values for bimetallic and monometallic catalysts under stoichiometric (CH_4:O_2:H_2O = 1:2(:100)) and oxygen excess (CH_4:O_2:H_2O = 1:120(:100)) methane oxidation conditions. The TOF was calculated using the activity at 250 °C for dry and 350 °C for wet conditions. All bimetallic catalysts have a total of 5 wt.% of Pd + Pt, so the 'bimetallic' 5 wt.% Pd catalyst contains no platinum. All catalysts were pretreated at a temperature 500 °C.

due to a reduced number of the active palladium sites. Nevertheless, there is a clear benefit to the addition of platinum under wet conditions, in both stoichiometric and oxygen-rich conditions.

Turnover frequencies, extracted from the activity measurements at 250 °C (dry) and 350 °C (wet) are presented in figure 3. TOF values are generally comparable to those reported for similar catalysts, ranging from 1×10^{-3} to 5×10^{-2} s^{-1} [4]. Under dry conditions—both stoichiometric and oxygen excess—an increase in Pd:Pt ratio gave a higher turnover frequency. Under wet conditions however there was significant variation, as the 4.0Pd–1.0Pt catalyst had a higher TOF than both the 2.5Pd–2.5Pt and 5.0Pd catalysts. Under stoichiometric wet conditions, the 2.5Pd–2.5Pt had a higher TOF than 5.0Pd, but a lower TOF under oxygen excess wet conditions. For monometallic palladium catalysts, the TOF values follow the same order as the average particle sizes: 5.0Pd < 2.5Pd < 4.0Pd, in line with earlier findings by Price *et al* for partial methane oxidation [35]. This trend was partially maintained under wet conditions, but with all catalysts having a lower turnover frequency, and 2.5Pd now showing a lower TOF than 5.0Pd.

When comparing monometallic and bimetallic catalysts with the same Pd loading, 2.5Pd had a higher TOF in both dry and wet (oxygen excess) conditions than 2.5Pd–2.5Pt, with a much larger difference under dry conditions. 4.0Pd however, had a lower TOF than 4.0Pd–1.0Pt, with a larger difference under wet conditions.

Near-ambient pressure XPS data for three catalysts, 5.0Pd, 4.0Pd–1.0Pt and 2.5Pd–2.5Pt, are presented in figure 4. All of these experiments were conducted under stoichiometric dry (0.11 mbar CH_4 + 0.22 mbar O_2) or wet (0.11 mbar CH_4 + 0.22 mbar O_2 + 0.22 mbar H_2O) conditions. At the start of each experiment, measurements were conducted in vacuum (below 1×10^{-7} mbar) at room temperature. These spectra show approximately 35%–40% Pd(II) for both the 5.0Pd and 4.0Pd–1.0Pt catalysts. The 2.5Pd–2.5Pt however is significantly more oxidised, with 87% Pd(II). This is consistent with various previous studies which suggests that Pt addition can be beneficial in preserving an oxidised state of palladium [22–24, 26]. Additionally, smaller Pd particles are more readily oxidised to PdO under reaction conditions [9]. With increasing temperature, in dry and wet conditions, significant changes in Pd(II) are observed for all catalysts.

The changes in oxidation state are summarised in figure 5, which overlays the fraction of Pd(II) (referred to here as Pd(II)%) as derived from NAP-XPS with the catalytic activity plots shown previously. In figures 5(a)–(c) this data is shown for 5.0Pd, 4.0Pd–1.0Pt, and 2.5Pd–2.5Pt catalysts respectively, under a total of 5 conditions per catalyst.

Under dry and low water stoichiometric conditions, the 4.0Pd–1.0Pt sample is more oxidised than the 5.0Pd sample at most relevant reaction temperatures. Both dry experiments show a significant drop in the percentage of Pd(II) during the reaction, for 5.0Pd this is from 85% Pd(II) at 177 °C (pre-reaction) down to 37% Pd(II) at 327 °C (near 100% conversion). After full conversion is reached, there is a significant re-oxidation, with 5.0Pd reaching 96% Pd(II) by 427 °C. This effect is reduced under wet (1:2:2) conditions, with the reduction not seen at all under very wet (1:2:100)

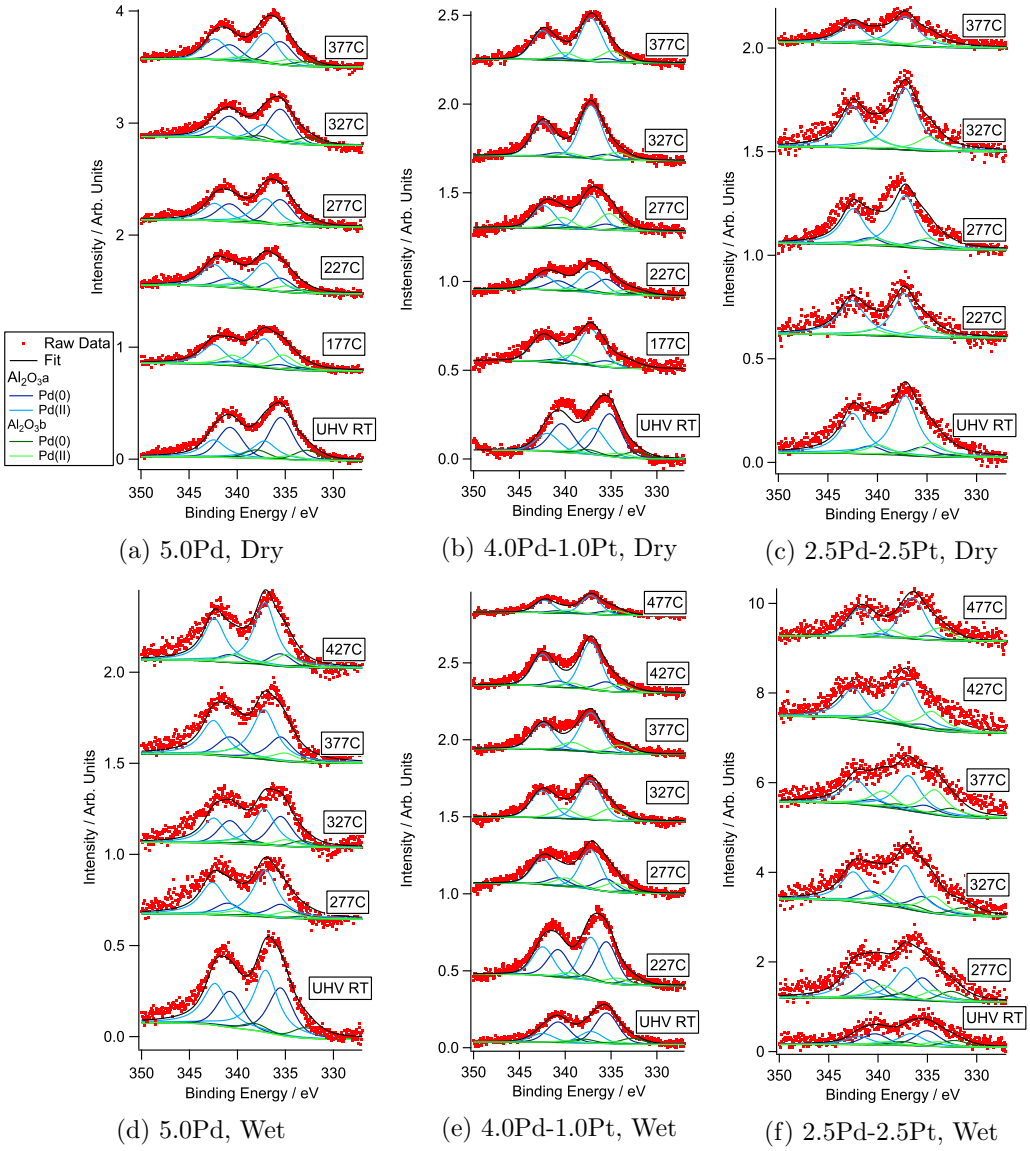

(a) 5.0Pd, Dry (b) 4.0Pd-1.0Pt, Dry (c) 2.5Pd-2.5Pt, Dry

(d) 5.0Pd, Wet (e) 4.0Pd-1.0Pt, Wet (f) 2.5Pd-2.5Pt, Wet

Figure 4. XPS spectra for a selection of Al_2O_3 supported catalysts, under stoichiometric dry (0.11 mbar $CH_4 + 0.22$ mbar O_2; CH_4:O_2:$H_2O = 1$:2:0) or wet (0.11 mbar $CH_4 + 0.22$ mbar $O_2 + 0.22$ mbar H_2O; CH_4:O_2:$H_2O = 1$:2:2) conditions. All catalysts were pretreated at a temperature 500 °C.

conditions. In general, wetter conditions lead to a lesser degree of oxidation at all temperatures, though between 327 °C and 377 °C there is only a minor difference. When measurements were carried out under very wet conditions at 477 °C, i.e. significantly above the point where 100% conversion was reached, the palladium is fully oxidised again. All NAP-XPS data recorded for the 5.0Pd sample indicate that, under any gas condition, the palladium will eventually be fully oxidised once a high enough temperature is reached. For 4.0Pd–1.0Pt however, all conditions seem to lead to a plateau in the palladium oxidation state, the level of which depends on the gas composition. In the case of oxygen rich gas feeds this plateau is at 100%. Under stoichiometric conditions the level decreases from ≈90% to ≈60% with increasing water content.

The data for the 2.5Pd–2.5Pt sample show a less clear relationship between reaction conditions and palladium oxidation state. At all temperatures, under dry conditions, the more oxygen rich gas feed leads to a less oxidised sample, which is contrary to expectations, however this effect is clearly seen in the comparison of the original Pd 3d data (see figure S8 of supporting information). This trend is reversed in a wet reaction mixture. The increase of water in the gas feed has a largely insignificant effect up to 377 °C, after which there are significant changes, which do not follow an obvious trend.

When looking at oxygen rich wet conditions, the 4.0Pd–1.0Pt sample is active at lower temperatures than the 5.0Pd. This comes at a point where it is comparatively less oxidised (86% compared to 100%). At higher temperatures, where both catalysts are equally oxidised, the 5.0Pd is slightly more active. This is easily rationalised as when the nature of Pd in both is the same, the catalyst with a higher loading will perform better. This experiment suggests that the optimal

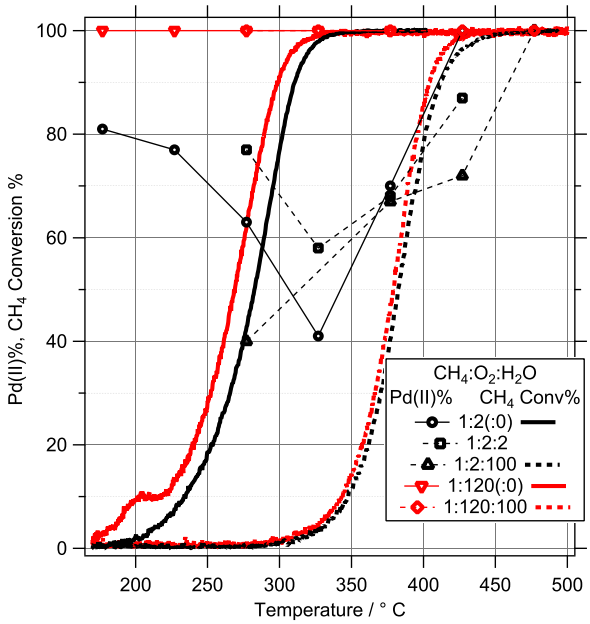

(a) 5 wt.% Pd

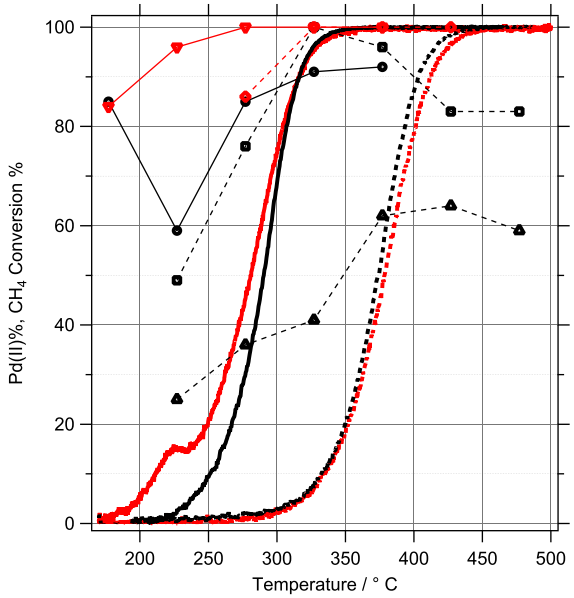

(b) 4 wt.% Pd + 1 wt.% Pt

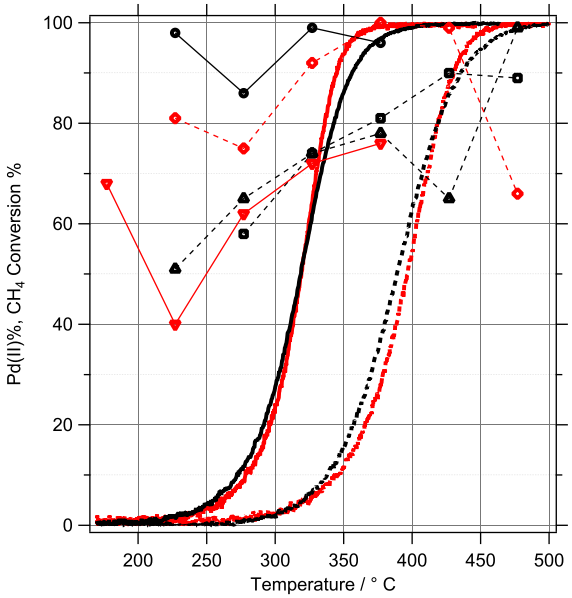

(c) 2.5 wt.% Pd + 2.5 wt.% Pt

Figure 5. Overlaid catalytic testing data with Pd(II)% as determined by NAP-XPS for a selection of Al_2O_3 supported catalysts. Data recorded under oxygen excess (CH_4:O_2:H_2O = 1:120(:100)) and stoichiometric (CH_4:O_2:H_2O = 1:2(:100) or 1:2(:2)) methane oxidation conditions. The data point at 327 °C for 5.0Pd under 1:2:100 conditions is omitted, due to a technical issue with that measurement. The data point presented at 477 °C for 2.5Pd–2.5Pt under 1:120:100 conditions is recorded on a different spot to the other measurements in those conditions. All catalysts were pretreated at a temperature 500 °C.

oxidation state of palladium for methane oxidation is not 100% Pd(II), but that there is a benefit from a partial presence of Pd(0). The dry oxygen rich conditions are largely consistent with expectations. Both 5.0Pd and 4.0Pd–1.0Pt being fully oxidised throughout most of the temperature range is consistent with the consistently weaker performance of the 4.0Pd–1.0Pt catalyst—as is expected from having a lower Pd loading.

Figure 6 shows laboratory XPS spectra for 5.0Pd, 2.5Pd–2.5Pt, and 5.0Pt catalysts, after calcination at 500 °C. The bimetallic sample shows no shift in the Pt 4d signal but a significant shift of +0.7 eV in the Pd 3d signal compared to the pure Pt and Pd samples, respectively. Although these spectra were recorded before the samples were exposed to reaction conditions, they indicate that Pd is more likely to oxidise than Pt in the bimetallic catalyst.

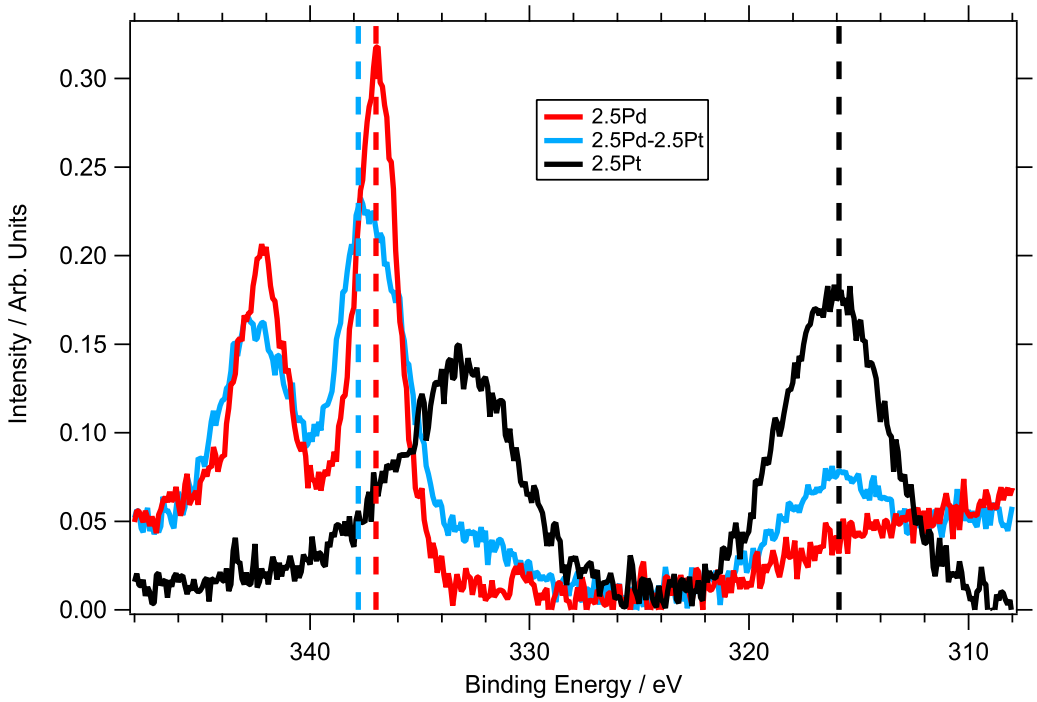

Figure 6. Pd 3d and Pt 4d region XPS data for monometallic 2.5Pd and 2.5Pt and bimetallic 2.5Pd–2.5Pt catalysts supported on Al_2O_3. All catalysts were calcined at 500 °C. Recorded with photon energy 1486.6 eV under UHV conditions at room temperature. Dashed lines are used to mark approximate peak positions.

4. Conclusions

Previous studies have shown that the support plays an important role in reducing the detrimental effects of water on Pd catalysts for methane oxidation [17, 19, 20]. In this study we have explored how the modification of the metal itself, namely the addition of platinum, a metal which on its own is a less active catalyst than palladium, can improve the catalytic activity of Pd catalysts under wet conditions.

From this study, there is a clear benefit to the addition of platinum to Pd/Al_2O_3 methane oxidation catalysts under stoichiometric conditions. Whilst at full conversion all catalysts were similarly oxidised—and as such the catalysts with higher Pd loadings perform best—there are significant differences at low temperatures. These differences in palladium oxidation state correlate well with increased activity/decreased deactivation. From TEM and EDX analysis, it is clear that the Pd–Pt are both present in the majority of particles, even after treatment at only 500 °C.

Analysis of turnover frequencies showed that under dry conditions (stoichiometric or oxygen excess), a Pd-rich Pd–Pt catalyst is preferable to Pt-rich or catalysts with equal amounts of both metals. This is consistent with previous experiments on Pd–Pt catalysts for methane oxidation, which have generally indicated that Pd should be present in a higher quantity than Pt [22, 23, 26].

Under dry conditions, catalysts with a higher Pd:Pt ratio also benefit more from a higher oxygen:methane ratio. Under wet conditions, however, a lower oxygen:methane ratio is beneficial to both bimetallic catalysts, but detrimental to the 5.0Pd monometallic. In dry or wet (oxygen excess) conditions, 4.0Pd had a higher TOF than 4.0Pd–1.0Pt, with a much larger difference in the dry condition. There is minimal difference between 2.5Pd–2.5Pt and 2.5Pd in wet conditions, though in dry conditions the TOF of 2.5Pd is much higher than the bimetallic catalyst. The fact that we observe a lower level of oxidised Pd in the dry oxygen-rich gas feed is unexpected and difficult to explain. A possible explanation is a kinetically hindered structural effect, such as fast encapsulation of particles by an oxide shell at low temperatures, which would prevent the core of the particle from oxidizing. It is worth noting that most earlier studies of similar systems do not change the CH_4:O_2 ratio and would therefore not have observed this effect [27–29].

In very oxygen-rich reaction mixtures there is a less clear benefit to the addition of Pt. Despite this, the tested 4.0Pd–1.0Pt catalyst lights off before the 5.0Pd catalyst under wet oxygen rich conditions, correlating with a relatively lower amount of Pd(II). It has previously been stated that a mixture of metallic and oxidised palladium is best for methane oxidation, and our experiments are largely in agreement with the optimal presence of Pd(II) being significant, but below 100% [40]. Equally, whilst a small addition of Pt is beneficial, as in 4.0Pd–1.0Pt, addition of larger amounts of Pt shows minimal benefit, largely due to the fact that Pd is removed. UHV XPS studies of powder catalyst systems showed a relative positive shift in palladium in a Pd–Pt catalyst compared to the Pd catalyst, suggesting that an increased oxidation state of Pd may be supported by the presence of Pt. However, under reaction conditions we do not consistently observe a higher level of Pd oxidation in bimetallic systems over pure

Pd. This leads to the conclusion that the origin of the superior properties of bimetallic Pd–Pt catalysts is more likely structural, i.e. related to particle size, shape, and/or surface composition, than electronic, i.e. related to the Pd oxidation state.

Acknowledgments

This work was carried out with the support of the Diamond Light Source, instrument B07 (Proposals SI19464, SI20952, SI22702, SI24584) and Swiss Light Source (SLS), Paul Scherrer Institute, Villigen, Switzerland, instrument NanoXAS (Proposal No. 20190527).

ORCID iDs

Alexander Large https://orcid.org/0000-0001-8676-4172
Jake Seymour https://orcid.org/0000-0002-1217-9541
Kanak Roy https://orcid.org/0000-0003-0802-7710
David C Grinter https://orcid.org/0000-0001-6089-119X
Luca Artiglia https://orcid.org/0000-0003-4683-6447
Kevin R J Lovelock https://orcid.org/0000-0003-1431-269X
Roger A Bennett https://orcid.org/0000-0001-6266-3510
Georg Held https://orcid.org/0000-0003-0726-4183

References

[1] Hicks R F, Qi H, Young M L and Lee R G 1990 *J. Catal.* **122** 280
[2] Muto K-i, Katada N and Niwa M 1996 *Appl. Catal.* A **134** 203
[3] Burch R R and Loader P K 1995 *Appl. Catal.* A **122** 169
[4] Gélin P and Primet M 2002 *Appl. Catal.* B **39** 1
[5] Monai M, Montini T, Gorte R J and Fornasiero P 2018 *Eur. J. Inorg. Chem.* **2018** 2884
[6] Firth J G and Holland H B 1969 *Trans. Faraday Soc.* **65** 1121
[7] McCarty J G 1995 *Catal. Today* **26** 283
[8] Pan Y X, Liu C J and Shi P 2008 *Appl. Surf. Sci.* **254** 5587
[9] Chin Y H C, García-Diéguez M and Iglesia E 2016 *J. Phys. Chem.* C **120** 1446
[10] Beck I E, Bukhtiyarov V I, Pakharukov I Y, Zaikovsky V I, Kriventsov V V and Parmon V N 2009 *J. Catal.* **268** 60
[11] Hellman A *et al* 2012 *J. Phys. Chem. Lett.* **3** 678
[12] Cullis C F, Nevell T G and Trimm D L 1972 *J. Chem. Soc. Faraday Trans.* 1 **68** 1406
[13] Burch R, Urbano F J and Loader P K 1995 *Appl. Catal.* A **123** 173
[14] van Giezen J C, van den Berg F R, Kleinen J L, van Dillen A J and Geus J W 1999 *Catal. Today* **47** 287
[15] Zhang F, Hakanoglu C, Hinojosa J A and Weaver J F 2013 *Surf. Sci.* **617** 249
[16] Barrett W, Shen J, Hu Y, Hayes R E and Scott R W J 2020 *ChemCatChem* **12** 944
[17] Velin P, Ek M, Skoglundh M, Schaefer A, Raj A, Thompsett D, Smedler G and Carlsson P A 2019 *J. Phys. Chem.* C **123** 25724
[18] Alyani M and Smith K J 2016 *Ind. Eng. Chem. Res.* **55** 8309
[19] Losch P, Huang W, Vozniuk O, Goodman E D, Schmidt W and Cargnello M 2019 *ACS Catal.* **9** 4742
[20] Murata K, Kosuge D, Ohyama J, Mahara Y, Yamamoto Y, Arai S and Satsuma A 2020 *ACS Catal.* **10** 1381
[21] Murata K, Mahara Y, Ohyama J, Yamamoto Y, Arai S and Satsuma A 2017 *Angew. Chem. Int. Ed.* **50** 15993–7
[22] Lapisardi G, Urfels L, Gélin P, Primet M, Kaddouri A, Garbowski E, Toppi S and Tena E 2006 *Catal. Today* **117** 564
[23] Yashnik S A, Chesalov Y A, Ishchenko A V, Kaichev V V and Ismagilov Z R 2017 *Appl. Catal.* B **204** 89
[24] Narui K, Yata H, Furuta K, Nishida A, Kohtoku Y and Matsuzaki T 1999 *Appl. Catal.* A **179** 165
[25] Persson K 2006 *Bimetallic palladium catalysts for methane combustion in gas turbines* (KTH Royal Institute of Technology)
[26] Persson K, Ersson A, Jansson K, Fierro J L and Järås S G 2006 *J. Catal.* **243** 14
[27] Osman A I, Abu-Dahrieh J K, Laffir F, Curtin T, Thompson J M and Rooney D W 2016 *Appl. Catal.* B **187** 408
[28] Abbasi R, Huang G, Istratescu G M, Wu L and Hayes R E 2015 *Can. J. Chem. Eng.* **93** 1474
[29] Xu P, Wu Z, Deng J, Liu Y, Xie S, Guo G and Dai H 2017 *Chin. J. Catal.* **38** 92
[30] Corro G, Cano C and Fierro J L 2010 *J. Mol. Catal. A: Chem.* **315** 35
[31] Sharma H N, Sharma V, Mhadeshwar A B and Ramprasad R 2015 *J. Phys. Chem. Lett.* **6** 1140
[32] Martin N M *et al* 2017 *Catal. Struct. React.* **3** 24
[33] Nilsson J, Carlsson P A, Martin N M, Adams E C, Agostini G, Grönbeck H and Skoglundh M 2017 *J. Catal.* **356** 237
[34] Goodman E D *et al* 2017 *ACS Catal.* **7** 4372
[35] Price R, Eralp-Erden T, Crumlin E, Rani S, Garcia S, Smith R, Deacon L, Euaruksakul C and Held G 2016 *Top. Catal.* **59** 516
[36] Pinna F 1998 *Catal. Today* **41** 129
[37] Held G *et al* 2020 *J. Synchrotron Radiat.* **27** 1153
[38] Orlando F *et al* 2016 *Top. Catal.* **59** 591
[39] Novotny Z *et al* 2020 *Rev. Sci. Instrum.* **91** 023103
[40] Huang F, Chen J, Hu W, Li G, Wu Y, Yuan S, Zhong L and Chen Y 2017 *Appl. Catal.* B **219** 73